Supplementary Material:
Emergent Spatial Coordination from Negative Selection Alone

Anonymous

Density Sweep Robustness

The main experiments use a fixed density of 7.5% (30 agents on a 20×20 grid). To assess robustness across density levels, we evaluated both Phase 1 and Phase 2 across 12 density conditions: 3 grid sizes (15×15, 20×20, 30×30) $\times$ 4 agent counts (15, 30, 60, 90), yielding densities from 0.017 to 0.400. Each condition was evaluated with 600 rules (100 rules $\times$ 6 seed batches), totaling 14,400 rule evaluations, all using the Miller-Madow bias-corrected MI estimator.

Table 1 and Figures 1 and 2 present the results. Phase 2 achieves nonzero median $\text{MI}_{\text{excess}}$ in 8 of 12 conditions, including all conditions with ≥ 60 agents, peaking near $d = 0.100$ ($\text{MI}_{\text{excess}} = 0.246$ bits at 30×30, 90 agents) before declining at higher densities. Phase 1 remains at zero median $\text{MI}_{\text{excess}}$ across all 12 conditions, confirming that the Phase 2 advantage is not an artifact of the specific grid configuration used in the main experiments.

Phase 2 also consistently achieves higher survival rates than Phase 1, with the gap widening at higher densities (e.g., 76.7% vs. 64.0% at $d = 0.225$; 83.7% vs. 68.0% at $d = 0.400$).

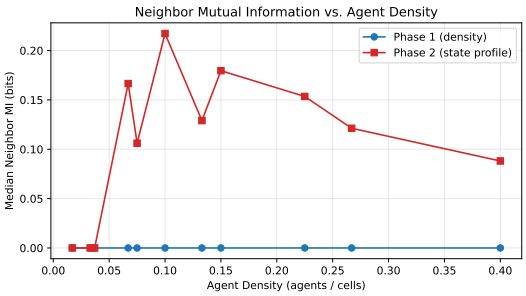

Figure 1: Median neighbor MI vs. agent density for Phase 1 and Phase 2. Phase 2 MI peaks at medium densities and declines at higher densities, while Phase 1 remains at zero throughout.

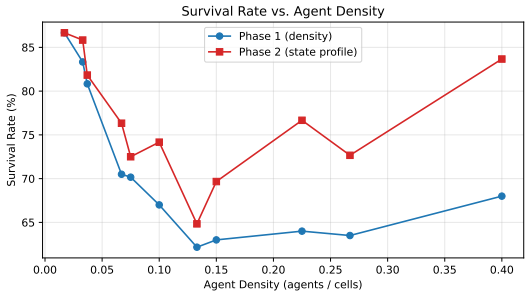

Figure 2: Survival rate vs. agent density. Phase 2 consistently achieves higher survival than Phase 1, with the gap widening at higher densities.

Multi-Seed Robustness

The main experiments evaluate each rule table with a single simulation seed. To assess whether $\text{MI}_{\text{excess}}$ levels are robust properties of the rule table rather than seed-specific accidents, we selected the top 50 rules by $\text{MI}_{\text{excess}}$ from each rule-based condition (Phase 2, Phase 1, and Control) and re-evaluated each across 20 independent simulation seeds.

Table 2 shows that 82% of top Phase 2 rules maintain positive median $\text{MI}_{\text{excess}}$ across seeds, and on average 73.3% of seeds per rule produce positive excess MI. In contrast, only 36% of top Phase 1 rules and 44% of top Control rules maintain positive median $\text{MI}_{\text{excess}}$, with mean positive fractions of 0.396 and 0.446 respectively. This confirms that MI differences across conditions reflect genuine rule properties rather than seed-specific accidents: Phase 2's elevated MI is robust, while Phase 1 and Control's lower MI levels are equally stable across seeds.

Moran's I by Condition

Table 1 in the main text reports the same-state adjacency fraction as the primary categorical spatial statistic. For completeness, we report Moran's I here, noting that it treats categorical states as numeric (computing

Table 1: Density sweep results across 12 conditions. MI_{excess} values are Miller-Madow corrected, bits. Phase 2 achieves nonzero median MI_{excess} in 8 of 12 conditions, including all conditions with ≥ 60 agents, while Phase 1 remains at zero across all densities tested.

Density	Grid	Agents	Median MI_{excess} (bits)		Survival (%)	
			P1	P2	P1	P2
0.017	30×30	15	0.000	0.000	86.7	86.7
0.033	30×30	30	0.000	0.000	83.3	85.8
0.037	20×20	15	0.000	0.000	80.8	81.8
0.067	15×15	15	0.000	0.000	68.7	76.0
0.067	30×30	60	0.000	0.199	70.5	76.3
0.075	20×20	30	0.000	0.114	70.2	72.5
0.100	30×30	90	0.000	0.246	67.0	74.2
0.133	15×15	30	0.000	0.130	62.2	64.8
0.150	20×20	60	0.000	0.191	63.0	69.7
0.225	20×20	90	0.002	0.176	64.0	76.7
0.267	15×15	60	0.000	0.148	63.5	72.7
0.400	15×15	90	0.000	0.107	68.0	83.7

Table 2: Multi-seed robustness of top-50 rules per condition (20 seeds each). Phase 2's elevated MI is a robust rule property; Phase 1 and Control's low/zero MI are equally stable across seeds.

Metric	Phase 2	Phase 1	Control
Rules with median $MI_{excess} > 0$	41/50 (82%)	18/50 (36%)	22/50 (44%)
Mean $P(MI_{excess} > 0)$ across seeds	0.733	0.396	0.446
Overall survival rate	76.2%	90.7%	78.7%

deviations from an arithmetic mean) and is therefore inappropriate as a primary indicator for nominal data.

Table 3: Median Moran's I by condition (final-step snapshot, 5,000 rules per condition). Moran's I treats states as numeric and is a secondary indicator; see Table 1 for the categorical adjacency fraction.

Condition	Median Moran's I
Random Walk	-0.030
Control	0.124
Phase 1	-0.011
Phase 2	-0.020

Halt Window Sensitivity

The main experiments use a 10-step halt window. To assess sensitivity, we evaluated the top-50 Phase 2 rules across halt windows of {5, 10, 20} steps.

Table 4: Halt window sensitivity for top-50 Phase 2 rules. Results are qualitatively unchanged across the tested range.

Halt Window	Survival Rate	Median $\text{MI}_{\text{excess}}$
5	78.0%	0.486
10	78.0%	0.486
20	78.0%	0.486

Table 4 confirms that the halt-window parameter has no impact on the qualitative findings for these top-performing rules: survival rates (78.0%) and median $\text{MI}_{\text{excess}}$ (0.486 bits) are identical across all three tested windows. This indicates that the top-50 rules either survive to completion or halt well within the first 5 steps, with no rules in the intermediate regime.

Survival Rates with Confidence Intervals

Table 5: Survival rates with Wilson score 95% confidence intervals (5,000 rules per condition).

Condition	Survived / Total	Rate	95% CI
Random Walk	5000/5000	100.0%	[99.9, 100.0]%
Control	2227/5000	44.5%	[43.1, 45.9]%
Phase 1	3571/5000	71.4%	[70.1, 72.7]%
Phase 2	3735/5000	74.7%	[73.5, 75.9]%

Random Walk $\text{MI}_{\text{excess}}$ Across Densities

To confirm that the random walk's $\text{MI}_{\text{excess}}$ remains near zero regardless of agent density, we extended the density sweep to include the Random Walk condition. Across all 12 density conditions (density range 0.017–0.400), the random walk produces $\text{MI}_{\text{excess}} \approx 0$ (median ≤ 0.06 bits), confirming that its elevated raw MI is entirely attributable to pair-count bias at all tested densities.

Alternative Null Models

In addition to the state-shuffle null used throughout the main text, we evaluated two alternative null models to assess the robustness of the MI calibration:

- Block shuffle: States are shuffled within spatial blocks (4×4), preserving local autocorrelation structure while destroying inter-block correlations.
- Fixed-marginal: Synthetic snapshots are generated with identical marginal state distributions but independent spatial placement (each position draws independently from the observed state frequencies).

Table 6: Alternative null model comparison for top-50 Phase 2 rules (mean MI across 200 null samples per rule). All three null models produce substantially lower MI than the observed values, confirming that Phase 2's elevated MI reflects genuine spatial coordination.

Null Model	Mean Null MI (bits)
State shuffle (main text)	0.264
Block shuffle (4×4)	0.899
Fixed-marginal	0.250

The block-shuffle null produces substantially higher MI (0.899 bits) than the state-shuffle null (0.264 bits), as expected since it preserves within-block correlations. The fixed-marginal null (0.250 bits) is comparable to the state-shuffle. In all cases, mean observed MI for the top-50 Phase 2 rules (1.646 bits) substantially exceeds the null values, confirming genuine spatial coordination.

Spatial Scrambling Control

To confirm that Phase 2's elevated MI depends on agents' specific positions rather than their state distribution alone, we performed spatial scrambling: for each rule's final snapshot, we randomly reassigned occupied positions among agents while keeping their states fixed ($N = 200$ scrambles per rule).

For top-50 Phase 2 rules, the mean observed MI is 1.646 bits while the mean scrambled MI drops to 0.270 bits—comparable to the shuffle null baseline (0.264 bits). This confirms that the observed MI arises from genuine local spatial coordination (agents with correlated states being near each other) rather than from the state distribution itself.

Transfer Entropy

Mutual information measures symmetric statistical dependence between neighboring states. To assess directional information flow, we computed transfer entropy (TE) from neighbor states to agent next-states:

$$\mathrm{TE} = I(S_j^t; S_i^{t+1} \mid S_i^t) \tag{1}$$

where S_i^t is agent i's state at time t and S_j^t is a neighboring agent's state. This measures how much knowing a neighbor's current state reduces uncertainty about the focal agent's next state, beyond what the agent's own current state provides.

Miller-Madow bias correction is applied. For the top-50 rules in each condition, median TE values are: Phase 2 = 0.072 bits, Phase 1 = 0.003 bits, Control = 0.113 bits. Phase 2 shows substantially elevated TE compared to Phase 1, confirming directional information flow from neighbors to agents. The Control condition's higher TE reflects its inclusion of a step-clock dimension that creates temporal state dependence without genuine spatial coordination (recall that Control $\mathrm{MI}_{\mathrm{excess}} \approx 0$).

Capacity-Matched Controls

To further isolate the role of observation content from table capacity, we evaluated two additional control conditions:

- Capacity-matched Phase 1: 100-entry tables where indices are aliased so that all dominant-state values for the same (self-state, neighbor-count) pair map to the same action. This provides Phase-2-sized tables with only Phase-1-level observation content.
- Random-encoding Phase 2: 100-entry tables with the same alphabet size as Phase 2, but the mapping from neighborhood configuration to observation index is randomly permuted. This tests whether the structure of the encoding matters beyond alphabet size.

The capacity-matched Phase 1 control produces median $\mathrm{MI}_{\mathrm{excess}} = 0.000$ (survival 71.4%), matching standard Phase 1 ($\mathrm{MI}_{\mathrm{excess}} = 0.000$) and well below standard Phase 2 ($\mathrm{MI}_{\mathrm{excess}} = 0.096$). This confirms that table capacity alone does not explain the Phase 2 advantage—Phase-1-level observations remain ineffective even with 100-entry tables. The random-encoding Phase 2 control produces median $\mathrm{MI}_{\mathrm{excess}} = 0.106$ (survival 75.1%), comparable to standard Phase 2, which is expected because the observation encoding (self-state, neighbor count, dominant state) is identical; only the table-entry ordering differs, which is irrelevant for randomly generated tables.

Algorithmic Pseudocode

Simulation loop (world.py:step()). At each of the 200 time steps:

1. Generate a random permutation of agent indices.
2. For each agent in order:
   (a) Observe local neighborhood (von Neumann, 4 cells).
   (b) Compute observation vector (s, n, d) or (s, n) depending on phase, where s = own state, n = occupied neighbor count, d = dominant neighbor state.
   (c) Look up action in shared rule table: $a = T[\mathrm{index}(s, n, d)]$.
   (d) Execute action: move (if target cell empty), change state, or no-op.

Filter checks (filters.py). After each step, check: (1) Halt: positions and states unchanged for 10 consecutive steps → terminate. (2) State uniform: all agents share the same state → terminate.

MI computation (metrics.py). For the final snapshot:

1. Enumerate all occupied neighbor pairs (right/down on torus, deduped).
2. Compute joint and marginal state distributions from pairs.
3. $\hat{I} = \sum p(s_i, s_j) \log_2 \frac{p(s_i, s_j)}{p(s_i)\, p(s_j)}$.
4. Apply Miller-Madow correction: $\hat{I}_{\mathrm{MM}} = \hat{I} - \frac{K_{\mathrm{joint}} - K_X - K_Y + 1}{2n \ln 2}$.
5. Clamp to ≥ 0.

Shuffle null (metrics.py). Repeat 200 times: permute states among fixed occupied positions, compute $\hat{I}_{\mathrm{MM}}$, average. $\mathrm{MI}_{\mathrm{excess}} = \max(\hat{I}_{\mathrm{MM}} - \overline{I}_{\mathrm{shuffle}}, 0)$.

Cross-Condition Metric Profiles

Beyond mutual information, the simulation records five additional metric families (seven individual metrics) at every time step. Table 7 reports final-step values for surviving rules across all four conditions. All pairwise comparisons (Mann-Whitney U, Holm-Bonferroni corrected) are significant at $p < 0.001$ for every metric.

Table 7: Cross-condition metric profiles (surviving rules, final-step values). Median [Q1, Q3] reported. All pairwise Mann-Whitney U tests (Holm-Bonferroni corrected) are significant at $p < 0.001$; effect sizes are reported in the text as signed Cliff's δ (positive means first-listed group > second-listed group).

Metric	Random Walk	Control	Phase 1	Phase 2
Compression ratio	0.178 [0.173, 0.180]	0.163 [0.158, 0.168]	0.160 [0.153, 0.168]	0.160 [0.153, 0.168]
Action entropy (mean)	3.141 [3.139, 3.143]	2.725 [2.555, 2.853]	0.621 [0.337, 0.958]	0.778 [0.445, 1.249]
Action entropy (var.)	0.000 [0.000, 0.000]	0.020 [0.008, 0.041]	0.152 [0.071, 0.234]	0.190 [0.112, 0.278]
Cluster count	29 [28, 30]	29 [28, 30]	26 [22, 29]	27 [24, 29]
Quasi-period. peaks	4 [3, 5]	15 [9, 19]	0 [0, 6]	2 [0, 7]
Phase trans. max Δ	0.266 [0.233, 0.309]	0.691 [0.572, 0.818]	0.211 [0.161, 0.327]	0.260 [0.173, 0.361]
State entropy	1.941 [1.897, 1.969]	1.157 [0.948, 1.446]	1.295 [0.922, 1.555]	1.438 [1.091, 1.693]

Role differentiation. The variance of per-agent action entropy (action_entropy_variance) captures the degree to which agents specialize into distinct behavioral roles. High variance indicates that some agents repeatedly select the same action while others explore diverse actions—a signature of emergent role differentiation. Phase 2 exhibits the highest action entropy variance (median 0.190), followed by Phase 1 (0.152), while Control (0.020) and Random Walk (< 0.001) show minimal differentiation. The Phase 1 vs. Phase 2 difference is significant (Cliff's $\delta = -0.185$, $p < 10^{-42}$), confirming that richer observations support greater role specialization.

Temporal signatures. Quasi-periodicity peak count and phase-transition max Δ capture temporal dynamics beyond the MI time-series snapshots in the main text. Control shows strikingly high quasi-periodicity (median 15 peaks) and phase-transition max Δ (median 0.691), far exceeding Phase 1 (0 peaks, 0.211) and Phase 2 (2 peaks, 0.260). This reflects Control's step-clock dimension, which drives periodic state cycling without genuine spatial coordination ($\text{MI}_{\text{excess}} \approx 0$). Phase 1 and Phase 2 show low quasi-periodicity, consistent with their spatially structured but temporally stable dynamics. The Phase 1 vs. Phase 2 difference in max Δ is significant (Cliff's $\delta = -0.119$, $p < 10^{-18}$), suggesting that Phase 2's richer observations produce slightly more dynamic temporal trajectories.

Cascaded Filter Analysis

The main experiments use only weak (viability) filters: halt detection and state uniformity. The codebase also implements medium-strength filters—short-period detection (period ≤ 2, checked over 8 snapshots) and low-activity detection (unique-action ratio < 0.2 over 5 steps)—which target dynamically trivial but non-halted simulations.

To assess how filter stringency affects the survivor pool, we re-ran all 5,000 rules per condition with both weak and medium filters enabled (same deterministic seeds, ensuring direct comparability). Table 8 reports the cascade survival counts.

Table 8: Cascade survival table: weak-only vs. weak+medium filters (5,000 rules per condition, same seeds). Medium filters further refine the survivor pool while the observation-richness ordering (Control < P1 < P2) persists.

Condition	Weak Only	Weak+Medium	Δ
Phase 1	3,571 (71.4%)	2,812 (56.2%)	−759
Phase 2	3,735 (74.7%)	2,906 (58.1%)	−829
Control	2,226 (44.5%)	1,915 (38.3%)	−311

Medium filters remove an additional 15–17% of rules in Phase 1 and Phase 2, and 6% in Control (which already has lower weak-filter survival). Crucially, the observation-richness ordering persists: Phase 2 retains the highest survival rate (58.1%) among medium-filter survivors, followed by Phase 1 (56.2%) and Control (38.3%). Furthermore, the median $\text{MI}_{\text{excess}}$ among Phase 2 medium-filter survivors is 0.153 bits, confirming that the MI advantage is not an artifact of lax filtering. Phase 1 and Control medium-filter survivors have median $\text{MI}_{\text{excess}} = 0$.

PR26 Follow-Up Reproducibility Summary

The post-merge PR26 follow-up bundle is tracked via manifest commit 63fa9b2e289fb605254545cd48d2e610a5bcf9f2 (Zenodo DOI: 10.5281/zenodo.18713158). The generated summaries report: filtered survival 63.55% vs. no-filter 100.00%, phase-2 Kendall median N/A, TE median 0.0719, TE-null median 0.0040, and TE-excess median 0.0581.

The dominant high-MI phenotype is low_signal (count 44), and synchronous ablation reports 3 phase-

pair summaries.

This archival bundle was generated with the full follow-up configuration (n_rules=5000, steps=200) used for manuscript-scale post-merge PR26 reproducibility. The phase-2 ranking-stability Kendall median is reported as N/A because the compared seed batches produce no shared surviving rule IDs (n_rules=0 overlap); this value is intentionally rendered as N/A (non-identifiable correlation), not as a numeric estimate.

Shuffle-Null Convergence

To verify that $N = 200$ shuffles is sufficient for a stable noise-floor estimate, we evaluated the mean shuffle-null MI ($\overline{\mathrm{MI}}_{\mathrm{null}}$) for the top-50 Phase 2 survivors across $N \in \{10, 25, 50, 100, 200, 500\}$ shuffles per rule. Figure 3 shows that the estimate stabilises by $N \approx 50$ and changes by less than 0.003 bits between $N = 100$ and $N = 500$, confirming that $N = 200$ provides an ample noise-floor estimate with comfortable margin.

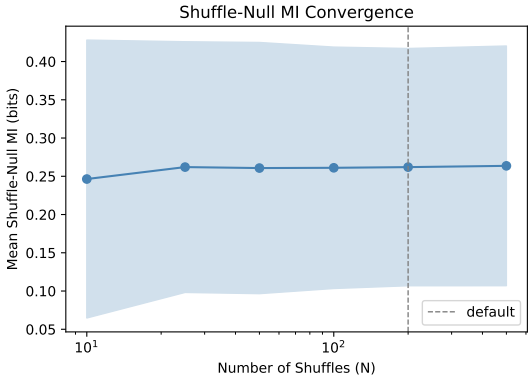

Figure 3: Shuffle-null MI as a function of shuffle count N for the top-50 Phase 2 survivors. Solid line: mean across rules; shaded band: ±1 SD. Dashed vertical line marks the default $N = 200$ used throughout.

Mutual Information as a Function of Pair Count

A potential confound is that Phase 2 rules produce more occupied adjacent pairs (n_{pairs}), which could mechanically increase MI estimates even under independence. To assess robustness, we computed median ΔMI within n_{pairs} bins {1–3, 4–6, 7–12, ≥ 13} across all four conditions (Figure 4). Phase 2 shows higher median ΔMI than Control and Phase 1 in every bin; it also surpasses Random Walk in the 4–6, 7–12, and ≥ 13 bins (where Phase 2 rules predominantly reside), confirming that the advantage is not an artifact of pair-count differences.

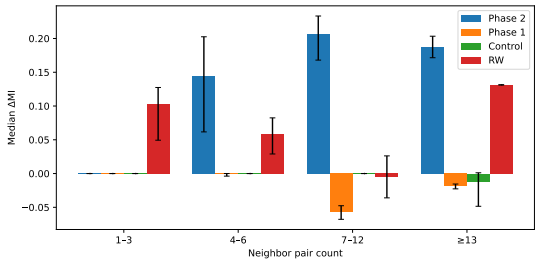

Figure 4: Median ΔMI (with 95% bootstrap CI) stratified by n_{pairs} bin for all four conditions. Phase 2's advantage persists within pair-count strata, ruling out pair-count as a confounding variable.

Population-Level ΔMI(t) Trajectories

To assess whether the final-snapshot MI advantage of Phase 2 reflects sustained temporal dynamics or an artefact of measuring coordination at a single fixed step, we computed the per-step calibrated ΔMI(t) across a random sample of 500 surviving rules per condition at timestep intervals $t \in \{0, 10, 20, \ldots, 190, 199\}$ (21 checkpoints total). At each checkpoint, the shuffle null is computed freshly from the recorded snapshot at that step ($N = 10$ shuffles; sufficient for tracking the sign and shape of the population median). Early-terminated rules are censored at their last recorded step (MI at last recorded step is used; no imputation). Figure 5 shows the median ΔMI(t) and interquartile range (IQR) across the 500 sampled rules per condition.

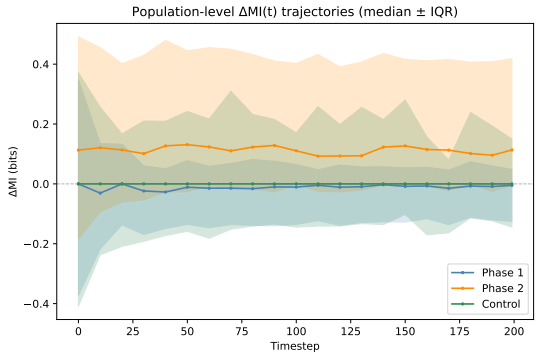

Figure 5: Population-level median ΔMI(t) ± IQR for 500 randomly sampled surviving rules per condition. Solid lines: median across rules at each timestep; shaded bands: 25th–75th percentile. Phase 2 (orange) remains above zero throughout all 200 steps (100% of timesteps with positive median); Phase 1 (blue) and Control (green) track at or below zero throughout (0% of timesteps with positive median). Censoring policy: early-terminated rules use MI at their last recorded step.

Phase 2's median $\Delta\text{MI}(t)$ is positive at 100% of the 21 timestep checkpoints; Phase 1 and Control achieve positive median $\Delta\text{MI}(t)$ at 0% of checkpoints. This demonstrates that the Phase 2 advantage is not an artifact of final-snapshot sampling: the population-wide calibrated coordination is positive and sustained throughout the simulation.

Archetype frequency by ΔMI quartile. To characterise what kinds of coordination rules produce across the full Phase 2 survivor distribution (n = 3,735), we applied the phenotype taxonomy (scripts/phenotype_taxonomy.py) to all surviving Phase 2 rules stratified by ΔMI quartile. Empirical medians: ΔMI = 0.142 bits, state entropy H_{state} = 1.438 bits (predictability fraction $0.142/1.438 \approx 9.9\%$). Results are shown in Table 9.

Table 9: Archetype counts per ΔMI quartile for all Phase 2 survivors (n = 3,735). Q1 = 0–25th percentile (ΔMI ≤ 0.056 bits); Q2 = 25–50th (0.056–0.142 bits); Q3 = 50–75th (0.142–0.437 bits); Q4 = 75–100th (> 0.437 bits). "Low-signal" is the residual category (ΔMI < 0.05, $H < 0.60$, or predictability < 0.40).

Archetype	Q1	Q2	Q3	Q4
Polarized cluster	0	0	0	0
Frozen patch	0	40	4	3
Mixed turbulent	0	5	37	58
Low signal	934	889	892	873

The low-signal category dominates all quartiles, confirming that the majority of Phase 2 survivors produce modest coordination. Frozen-patch rules (static correlated structures) peak in Q2 (median-range ΔMI); mixed-turbulent rules (dynamic state propagation) are most prevalent in Q3–Q4 (upper half). Critically, the top-ΔMI quartile (Q4) contains no polarized-cluster rules, consistent with the anti-correlated boundary interpretation: high-ΔMI rules exhibit near-zero same-state adjacency fraction, indicating anti-correlation rather than same-state clustering.

Distribution-Wide Multi-Seed Robustness

Supplementary §B evaluates multi-seed robustness for the top-50 Phase 2 rules by ΔMI. Here we extend the analysis to 200 randomly selected surviving rules per condition (uniform random sample, not selected by ΔMI), re-evaluating each rule across 10 independent initial seeds. To quantify sampling uncertainty, we repeat this procedure with $B = 5$ independent random samples (RNG seeds 0–4) and report bootstrap confidence intervals across resamples. Control is excluded because rule seeds are not available in the experiment log for that condition.

Table 10: Distribution-wide multi-seed robustness ($B = 5$ resamples of 200 random survivors, 10 seeds per rule). Fraction positive median: fraction of rules whose median ΔMI > 0 across seeds. Mean $P(\Delta\text{MI} > 0)$: mean fraction of seeds with ΔMI > 0. 95% CI is the percentile interval across $B = 5$ resamples.

Condition	Frac. pos. med. [95% CI]	$\overline{P}(\Delta\text{MI}>0)$ [95% CI]
Phase 1	0.265 [0.230, 0.310]	0.326 [0.310, 0.351]
Phase 2	0.709 [0.680, 0.730]	0.646 [0.627, 0.669]

The Phase 2 fraction with positive median ΔMI (70.9%) is substantially higher than Phase 1 (26.5%), with non-overlapping 95% bootstrap CIs. This confirms that seed robustness is a property of the full Phase 2 survivor distribution, not only the top performers: a random draw of 200 Phase 2 survivors exhibits the same qualitative ordering as the top-50 results in §B (Phase 2: 84%, Phase 1: 36% among top-50).

Synchronous Update Ablation

To assess whether the Phase 2 coordination advantage depends on sequential update order, we re-ran all 5,000 rules per condition under synchronous update semantics (all agents act simultaneously using the previous step's state). Table 11 reports the median ΔMI, Cliff's δ, corrected p-value, and survival rate for each condition under both update modes.

Table 11: Synchronous vs. sequential update ablation. Cliff's δ (sequential vs. synchronous); p_{corr} is Holm-Bonferroni corrected. Phase 2 retains positive median ΔMI under synchronous updates (0.013 bits vs. 0.096 bits sequential); Phase 1 and Control remain at zero.

Condition	Seq. ΔMI	Sync. ΔMI	p_{corr}
Phase 1	0.000	0.000	0.797
Phase 2	0.096	0.013	1.6×10^{-9}
Control	0.000	0.000	—

The Phase 1 and Control conditions show no significant difference between update modes (Phase 1: Cliff's $\delta = 0.002$, $p_{\text{corr}} = 0.797$). Phase 2's median ΔMI is reduced approximately 7-fold under synchronous updates (0.013 vs. 0.096 bits), but remains positive, confirming that the directional result (P2 > P1 = Control) is preserved. The magnitude reduction is consistent with synchronous update eliminating the implicit temporal ordering that allows state-propagation rules to propagate information across multiple agents in a single step.

Termination Mode Breakdown

Table 12 breaks down how each of the 5,000 rules per condition terminates. Halt detection fires when all agents' positions and states are unchanged for $W = 10$ consecutive steps; state-uniformity fires when all 30 agents share the same internal state. For the Control condition, the termination mode is not separately logged; the 2,773 non-surviving rules are reported as "not recorded."

Table 12: Termination mode counts per condition ($n =$ 5,000 per condition). State-unif. = state-uniformity termination; N/R = not separately recorded (Control only).

Condition	Survived	Halt	State-unif.	Total
Phase 1	3,571 (71.4%)	931 (18.6%)	498 (10.0%)	5,000
Phase 2	3,735 (74.7%)	916 (18.3%)	349 (7.0%)	5,000
Control	2,227 (44.5%)	N/R	N/R	5,000

Control is disproportionately terminated relative to the rule-based conditions (55.5% non-survival vs. 28.6% for Phase 1 and 25.3% for Phase 2). This is consistent with the Control step-clock producing globally synchronised state oscillations that rapidly drive agents to uniform state when the clock cycle aligns across all agents.

Full-distribution ΔMI (survived + terminated). To confirm that termination does not create a selection artefact, we compute ΔMI at each rule's last recorded step for all 5,000 rules per condition (censoring policy: MI at last recorded step, no imputation). Table 13 reports the full-distribution results.

Table 13: Full-distribution ΔMI (all 5,000 rules per condition; MI at last recorded step for terminated rules). The condition ordering Phase 2 > Phase 1 $\approx$ Control is preserved even when terminated rules are included.

Condition	Median ΔMI	Fraction ΔMI > 0
Phase 1	0.000	28.6%
Phase 2	0.096	58.0%
Control	0.000	14.4%

The Phase 2 median ΔMI remains 0.096 bits in the full distribution (identical to the survivor-only value, because the terminated rules have near-zero ΔMI on average and do not shift the median substantially). Phase 1 and Control retain median ΔMI = 0. State-uniformity filtering removes only zero-MI configurations and cannot preferentially select high-MI survivors.

References